Effective boundary extrapolation length to account for finite-size effects in the percolation crossing function

Robert M. Ziff
Department of Chemical Engineering, University of Michigan, Ann Arbor, Michigan 48109-2136
(Received 8 March 1996)

The crossing probability function $\pi_v(H,W,p)$ for bond percolation on a square lattice with rectangular boundaries up to $H\times W=1024\times 256$ in size is determined numerically to high precision using a hull-walk simulation technique. At $p=p_c$ it is found that the finite-size corrections to Cardy's formula can be accurately accounted for simply by assuming that the effective aspect ratio of the system is $r_{\rm eff}=(H+h)/(W+w)$ with $h\approx w\approx 0.36$, without any additional correction terms. The constants h and w are essentially twice the extrapolation lengths to the effective location of the boundary by the continuum percolation field. Results for π_v at $p\neq p_c$ and for $\partial\pi_v/\partial p$ at p_c verify that $\pi_v(H,W,p)$ scales as $\pi_v^{(1)}(H/W,(p-p_c)W^{1/\nu})$ or equivalently as $\pi_v^{(2)}(H/W,(p-p_c)(HW)^{1/2\nu})$. [S1063-651X(96)13609-6]

PACS number(s): 64.60Ak, 05.70.Jk

I. INTRODUCTION

The function $\pi_v(p)$, which gives the probability of crossing a rectangular system between opposite boundaries in (say) the vertical direction, is central to the theory of percolation. In the limit of an infinitely large system, $\pi_v(p)$ goes over to a step function, demonstrating the discontinuous nature of the percolation process and defining its transition point p_c exactly. For finite systems, the behavior of $\pi_v(p)$ near p_c reflects finite-size scaling, and is relevant to renomalization-group (RG) theory.

The behavior of this function has been the subject of numerous investigations over the years. Bernasconi [1] showed that a properly defined square boundary for bond percolation on a square lattice produces a perfectly symmetric function $\pi_v(p)$ about the point $p=\frac{1}{2}$ for systems of all size L, implying $\pi_v(p_c)=p_c=\frac{1}{2}$ when $L\to\infty$. This result is supportive of the one-parameter RG construction $\pi_v(p_{\rm RG})=p_{\rm RG}$ first proposed by Young and Stinchcombe [2], since in this case the RG gives the critical point exactly. Extensive Monte Carlo simulations of $\pi_v(p)$ for various systems have been carried out by many authors, starting with Kirkpatrick [3] and Reynolds, Stanley and Klein [4]. The latter authors [4] also introduced a variety of important estimates of p_c for finite systems that derive from $\pi_v(p)$ [which they call $R(p)$], including $p_{\rm av}$, the average p under the distribution $\partial\pi_v/\partial p$; $p_{\rm max}$, the maximum in this distribution; and p_{c-c}, the cell-to-cell RG fixed point; as well as the RG fixed point $p_{\rm RG}$. Stauffer and co-workers investigated percolation in many situations using a method in which the distribution of values of p where percolation first occurs is determined; that distribution is precisely $\partial\pi_v/\partial p$ [see [5], where $\Pi(p)$ is used to indicate the crossing probability]. In more recent work, Hu and co-workers developed a Monte Carlo histogram technique that allows $\pi_v(p)$ [which Hu called the existence probability $E(p)$] to be efficiently determined over a wide range of p [6–10]. Monetti and Albano studied a criterion for percolation related to the crossing probability (which they called the percolation probability P.P.(p)] for some rectangular systems [11]. Note that the crossing probability is also called $P(p)$ and $p'(p)$; the notation $\pi_v(p)$ has become especially common in the mathematical literature on this subject [12–14] and is adopted here.

In the past few years there has been particular interest in the behavior of π_v at and near the infinite system critical threshold p_c. Langlands and co-workers [12,13] carried out extensive Monte Carlo simulations for rectangular systems of various sizes and aspect ratios r (equal to the height divided by width), and Cardy [14] developed an exact theoretical formula for $\pi_v(r,p_c)$ for the case of free boundary conditions on the left and right sides, in the limit of infinitely large systems, using conformal invariance theory. Cardy found good agreement between his predictions and the numerical results of Langlands and co-workers, with some small deviations which he attributed to finite-size effects. In [15] we showed that Cardy's formula can be written in an explicit convergent series form, the first three terms of which yield

$$\pi_v^C(r,p_c) = \begin{cases} b\left(e^{-\pi r/3}-\frac{4}{7}e^{-7\pi r/3}+\frac{2}{13}e^{-13\pi r/3}\cdots\right), & r\leqslant 1 \\ 1-b\left(e^{-\pi/3r}-\frac{4}{7}e^{-7\pi/3r}+\frac{2}{13}e^{-13\pi/3r}\cdots\right), & r\geqslant 1, \end{cases} \tag{1}$$

where $b=2^{4/3}3\Gamma(\frac{2}{3})/\Gamma(\frac{1}{3})^2\approx 1.426\,348\,256$, and the superscript C is used here to indicate Cardy's result explicitly; these three terms are sufficient to calculate π_v to at least eight significant figures for all r.

In general, $\pi_v(r,p_c)$ for an infinite system is a universal quantity that is independent of the underlying lattice and type of percolation, but dependent upon the type of boundary condition on the sides and upon the dimensionality. Thus the type of lattice does not affect the asymptotic universal behavior (as long as the lattice has an isotropic scale), but it does influence the nature of the finite-size corrections. For the study of the latter, each system has to be investigated independently.

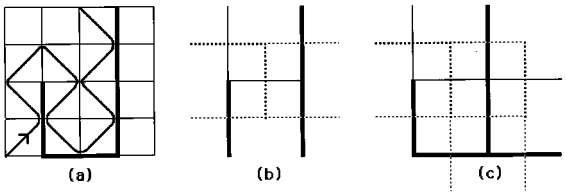

FIG. 1. (a) The hull-generating walk for bond percolation on a square lattice. (b) The construction of the equivalent hull configuration on the bond lattice, with heavier lines representing occupied bonds. The dual lattice is also shown by dotted lines, with the heavier ones representing dual-lattice bonds. (c) An alternative representation of the bond lattice that is often used; the dangling bonds on the right-hand side do not contribute to vertical percolation, but are useful to make a more symmetric duality construction as shown.

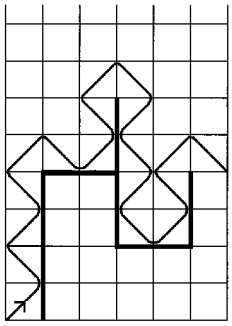

FIG. 2. The hull walk on a rectangular system of high aspect ratio. Keeping track of the maximum height that the walk reaches before being trapped on the right-hand side allows π_v to be determined for all H.

In [16], the author investigated $\pi_v(p_c)$ for site percolation on a square lattice within square systems of different sizes $L\times L$, both analytically for $L\leqslant 7$ and numerically for larger L. It was found that $\pi_v(L,p_c)\to\frac{1}{2}$ as $L\to\infty$, with an apparent correction of order $1/L$. In [16] it was also pointed out that the result $\pi_v(p_c)=\frac{1}{2}$ evidently conflicts with the predictions of a RG analysis, since the RG fixed point $(\pi_{\rm RG},p_{\rm RG})$ limits to (p_c,p_c), where $p_c=0.592\,746\ldots$ when $L\to\infty$, and therefore predicts that π_v should be $0.592\,746\ldots$ instead of $\frac{1}{2}$. However, as discussed in [17] and [18] and more recently in [19], this conflict more accurately concerns the single-parameter RG theory or the position-space RG, rather than the complete formal RG theory which can include ''irrelevant'' variables as well as normal finite-size effects. In any case, the one-parameter RG fixed point *cannot* in general be used to determine π_v. In [16] it was also shown that different estimates of p_c deduced from $\pi_v(p)$ for finite systems behave quite differently, and, in particular, that $p_{\rm av}$, $p_{\rm max}$, p_{c-c}, and other estimates converge to p_c an order of L more quickly than $p_{\rm RG}$ does *for this particular system* (site percolation, square lattice, square boundary, free sides). This rapid convergence for some of these quantities was observed (but not well understood) previously [4,20]. Further work on the question of $\pi_v(p_c)$ for different boundary conditions and higher-dimensional systems has been recently carried out [21–24].

In a very recent publication — while the present work was being completed — Hovi and Aharony [19] reported on extensive work investigating and expanding upon the points first put forth in [17]. One of the main predictions in [17] was that a confluent singularity yields a leading finite-size correction term of order $L^{-\vartheta_1}$ to π_v, where $\vartheta_1\approx 0.85$. However, these authors also allowed for the analytic corrections of order L^{-1} as suggested in [16], so the existence of the confluent term is difficult to show numerically. In [19] Hovi and Aharony provided some numerical evidence that the confluent term is necessary, for the case of site percolation on square systems (see especially their Fig. 5), but in our opinion the existence of such a term has not been shown unequivocally.

In the present work we investigate bond percolation on a square lattice with rectangular system boundaries over a continuous range of aspect ratios. We consider a vertical crossing and assume free boundary conditions on the two sides (rule R_1 of [4]). We find π_v by a simple hull-generating random walk that yields results simultaneously for rectangles of all widths W and heights H from a single simulation. For the behavior at $p=p_c$, we show that very precise agreement with Cardy's analytical formula can be achieved by using an effective lattice-boundary offset constant for both the width and height dimensions; no additional correction terms of the type proposed by Aharony and Hovi appear to be necessary. These lattice offset constants represent a continuum extrapolation length to the effective location of the boundary, and introduce analytic correction terms of order $1/W$ into π_v (except when $H=W$, when these finite-size corrections disappear for bond percolation). We also carry out simulations of π_v at $p\neq p_c$ and of $\partial\pi_v/\partial p$ at p_c, and find that the expected scaling behavior can be achieved to high precision by including only the lattice offset constants.

II. ALGORITHM

Hull walks were first introduced in [25] for site percolation, and in [26] for bond percolation on square lattices (also see walks of Gunn and Ortuño [27] and Ruijgrok and Cohen [28], and references in [29]). That hull walks can be used to find π_v directly was first pointed out by Grassberger [30]. Our previous simulations [16] considered the case of site percolation only. Here we consider bond percolation, on a square underlying lattice.

The procedure for finding π_v for this system is illustrated in Fig. 1. The walk takes place on a square lattice whose sites are at the *centers* of the bonds on the actual percolation lattice. The walker begins at the lower-left-hand corner of this lattice and moves only along diagonals. At each site it turns by 90°, either in the counter-clockwise (CCW) direction with probability p or the clockwise (CW) direction with probability $1-p$, except when a site has previously been visited, in which case the walker always turns either CW or CCW so as not to cross its path (a "kinetic self-avoiding trail" [31,32]). The bottom and left-hand boundaries of the system are reflecting, and the top and right-hand boundaries are adsorbing and terminate the walk.

This walk generates a path that bounces back and forth between the centers of the occupied bonds of the hull and the centers of the vacant bonds surrounding the hull (or equivalently the bonds on the dual lattice); turning CCW corre-

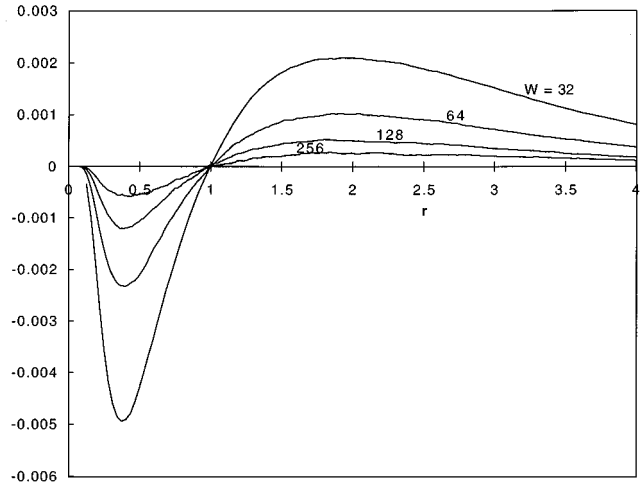

FIG. 3. A plot of $\pi_v(H,W,p_c)-\pi_v^{\mathrm{C}}(r,p_c)$ vs $r=H/W$, showing a discrepancy with Cardy's formula due to finite-size effects.

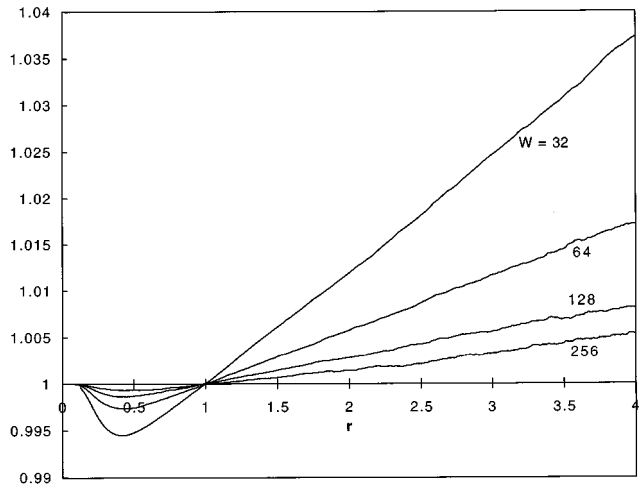

FIG. 4. A plot of $\pi_v(H,W,p_c)/\pi_v^{\mathrm{C}}(r,p_c)$ vs r, showing that the relative discrepancy increases with increasing r.

sponds to hitting an occupied bond, and CW a vacant or dual-lattice bond. If the top boundary is reached first, then the underlying bond system has percolated top-to-bottom as shown in Fig. 1, while if the right-hand side is first reached, then it has not (or, equivalently, the dual lattice has percolated left to right), as shown in Fig. 2 for a rectangular system. Clearly, by the symmetry of this construction, the crossing probability must be exactly one-half for square systems of any size when $p=\frac{1}{2}$, in agreement with Bernasconi's result. In the example shown in Fig. 1, with a 5×5 simulation lattice, one effectively simulates bond percolation on the 2×2 bond lattice shown in Figs. 1(b) or 1(c). To denote the lattice size in this paper, the bond dimensions (2×2 in this case) will be used.

To generalize this method to rectangles in a way that allows all aspect ratios to be considered simultaneously, we carry out this walk on a rectangular system of high aspect ratio, keeping track of the maximum height the walk attains before reaching the right-hand side, as shown in Fig. 2. Systems of height less than this maximum walk height percolate top to bottom, while those of greater height do not. Thus, by accumulating the number of runs in which the maximum height ranges from H to the maximum of the system, we determine the probability of percolating for a system of height H. Furthermore, in the same simulation we keep track of the rightmost position that the walk has gone, and in doing so also find $\pi_v(H,W,p)$ for all widths W. A sample program and explanation which describes in detail how this is carried out is available from the author [33].

The simulations were performed on an actual lattice of dimensions 2048×512 lattice points, which represents a bond lattice of $H\times W=1024\times 256$. The random number generator that was used is described in the Appendix. While the procedure in principle allows the determination of $\pi(H,W,p_c)$ for all H and W up to these maximum values, the resulting output would be rather large, so we retained data only for $W=32$, 64, 128, and 256, and $H\leqslant 4W$.

III. RESULTS

A. Comparison with Cardy's formula at $p=p_c$

A sample of 100 000 000 systems was simulated at $p=p_c=\frac{1}{2}$, requiring a few weeks of time on a workstation computer. The results are plotted in relation to Cardy's formula in Figs. 3–5.

In Figs. 3 and 4 we show the difference and ratio, respectively, of the two quantities $\pi_v(H,W,p_c)$ and $\pi_v^{\mathrm{C}}(r,p_c)$, as a function of $r=H/W$, for the four values of W. While the difference in Fig. 3 is small and goes to zero for large r, as observed by Cardy [14] using the data of Langlands *et al.* [12] (with much lower precision than given here), the ratio in Fig. 4 is seen to increase linearly with increasing r with a slope that depends upon system size. Although larger systems have lower slopes and give closer agreement with theory, clearly for a system of any finite size that ratio can be made arbitrarily large by making r sufficiently large.

The deviations shown in Figs. 3 and 4 are finite-size effects which we attribute to an uncertainty in the size of the system, or equivalently in the location of its boundary. To account for this uncertainty, we consider that the effective aspect ratio should not be simply H/W but instead be given by

$$r_{\mathrm{eff}}=(H+h)/(W+w), \tag{2}$$

where h and w are phenomenological constants. These constants represent a correction for the discretization of continuum space by a lattice and can be interpreted as twice the distance to the effective location of the boundary, extrapolated from the continuumlike behavior found deep within the system. This length is analogous to the extrapolation length that appears when relating discrete random walks to continuum diffusion in a system with an adsorbing boundary [34], and the Milne extrapolation length that appears in neutron adsorption. For such an idea to make physical sense, h and w should be of order of the lattice spacing, and should be independent of lattice size for larger lattices. They will, how-

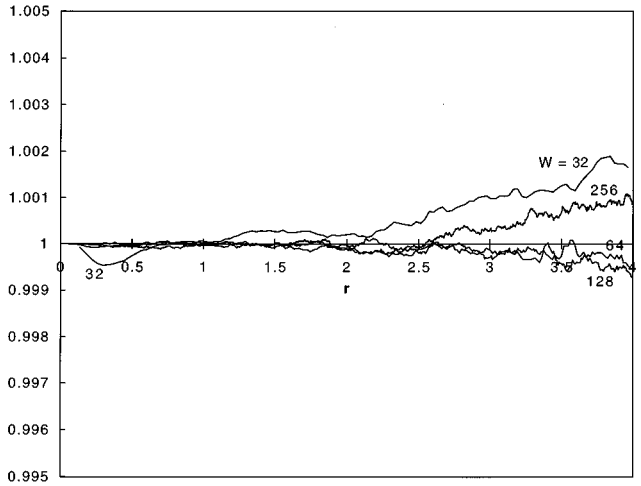

FIG. 5. A plot of $\pi_v(H,W,p_c)/\pi_v^{\mathrm{C}}(r_{\mathrm{eff}},p_c)$ vs $r_{\mathrm{eff}} = (H+h)/(W+w)$ with $h=w=0.36$. The deviations from unity for $W=64$, 128, and 256 are within statistical error, while those for $W=32$ at $r<1$ are small but statistically significant. Their vertical scale here is magnified five times over that of Fig. 4.

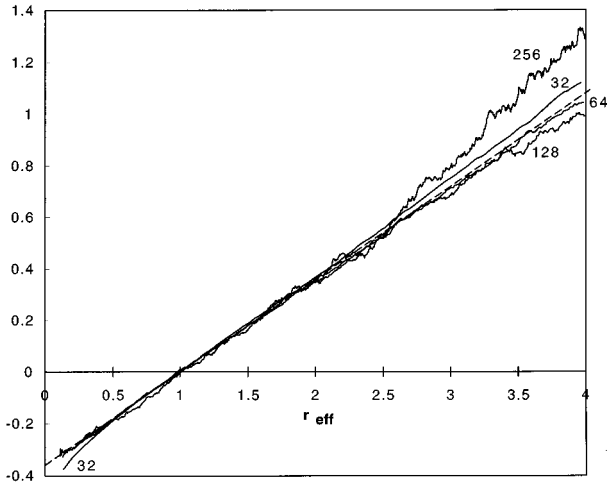

FIG. 6. A plot of $H-r_{\mathrm{eff}}W$ vs r_{eff} calculated from the measured values of π_v through (3). The dashed line has slope and negative intercept of 0.36.

ever depend upon the choice of lattice, percolation type (site or bond), and boundary condition.

Figure 5 shows the results when r_{eff} is used in place of r, taking $h=w=0.36$. Now, in contrast to what was seen in Fig. 4, the agreement between the simulation and theoretical results is within statistical error, except for small deviations for $W=32$. However, deviations for such small W are expected, and these results show that W need only be of order 100 for an infinite system to be very accurately approximated, if r_{eff} is used for the aspect ratio.

The value 0.36 for h and w was determined both empirically [adjusting to get the best agreement with (1)] and by the following procedure. For each measured value of $\pi_v(H,W,p_c)$, the corresponding value of the effective aspect ratio r_{eff} was determined from the inverse of (1):

$$r_{\mathrm{eff}}=\begin{cases} -\dfrac{3}{\pi}\ln(t+\frac{4}{7}t^7+\frac{194}{91}t^{13}\ldots), & \pi_v\leqslant\frac{1}{2} \\ -\left[\dfrac{3}{\pi}\ln(u+\frac{4}{7}u^7+\frac{194}{91}u^{13}\ldots)\right]^{-1}, & \pi_v\geqslant\frac{1}{2}, \end{cases} \tag{3}$$

where $t=\pi_v/b$, and $u=(1-\pi_v)/b$. These values of r_{eff} were used to construct a plot of $H-r_{\mathrm{eff}}W$ versus r_{eff}. Because (2) implies $H-r_{\mathrm{eff}}W=-h+r_{\mathrm{eff}}w$, it follows that such a plot should yield a straight line with slope w and intercept $-h$. The results of this plot for the four values of W are shown in Fig. 6. The data fall nicely on a single straight line, verifying (2), and yield $h\approx w\approx 0.36$ within an error of about ± 0.01. It is consistent with these data to take h and w equal to each other, which allows $\pi_v(W,W,p_c)=\frac{1}{2}$ to be satisfied exactly. Note that this choice makes the fitted line through the data in Fig. 6 pass precisely through the point (1,0).

While fixing $h=w$ thus guarantees that π_v at $r=1$ is matched exactly, it does not necessarily follow that the large-r behavior of π_v could also be simultaneously fit. This is because the asymptotic behavior of π_v for large r is of the form $B\exp(-Ar)$, with A and B differing slightly from their asymptotic values $\pi/3$ and b, respectively, for finite systems. By substituting $r_{\mathrm{eff}}=r/(1+w/W)+h/(W+w)$ in place of r in this exponential, it can be seen that in general one might have to adjust h and w independently to fit both the coefficient and decay of the leading exponential term precisely. Nevertheless, we found that an excellent fit of the large-r behavior could be achieved with $h=w$. For $r<1$, some deviations for the smallest lattice are apparent, and the data for this range are hardest to fit by (2). For even smaller lattices, it may be necessary to allow $h\neq w$ in order to fit the large-r behavior well, in which case the value for $r=1$ would not be matched precisely. However, this would be for quite small lattices where finite-size corrections are not expected to be simple. Note that the correction term proposed by Aharony and Hovi [17] would also not be useful here, since it would have its strongest effect on larger, not smaller, systems, relative to the $1/W$ correction implied by (2).

The above results imply that the large-r behavior of the curves in Fig. 4 should be $\exp(-\pi r_{\mathrm{eff}}/3)/\exp(-\pi r/3) = \exp[-(\pi/3)(rw-h)/(W+w)] \approx 1+\pi rw/3W$ for large W, or linear with slope $\pi w/3W\approx 0.377/W$. The slopes of the lines in Fig. 4 agree with this formula.

The use of (2) implies that the effective lattice dimensions are larger than the actual ones by the amounts h and w. For the case of bond percolation with free boundaries on the sides, the lattice dimensions are thus effectively 0.36 greater in each dimension, or, equivalently, the extrapolation of the percolation field to where it reaches the zero value overhangs the boundary by 0.18 lattice spacing on each of the four sides. Thus, for example, a 100×100 bond percolation system is effectively 100.36×100.36 in size, and therefore still has an effective aspect ratio of unity. A 200×100 system is effectively 200.36×100.36 in size, and has an effective aspect ratio 1.9964, while a 201×100 system has an effective aspect ratio of 2.0064. Note that no finite-size system has an effective aspect ratio of exactly 2.

The use of r_{eff} also implies that the corrections to $\pi_v(r)$ are analytic. To see this, write (2) as $r_{\mathrm{eff}}=r+\delta$, where $\delta=(h-rw)/(W+w)$, and expand the crossing function about the nominal value of the aspect ratio $r=H/W$:

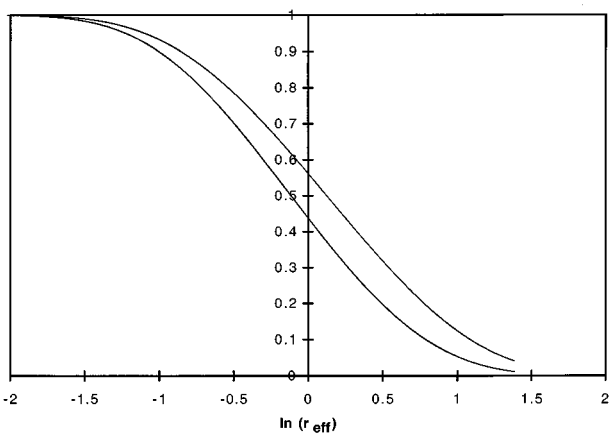

FIG. 7. A plot of $\pi_v(H,W,p)$ vs $r_{\rm eff}$ for the four parameter values (W,p) = (256,0.501), (128,0.501 682), (64,0.502 828), and (32,0.504 757) [all satisfying $(p-p_c)W^{1/\nu}=-0.064$], which are collapsed to the upper curve, and for the four values (W,p) = (256,0.499), (128,0.498 318), (64,0.497 172), and (32,0.495 243) [all satisfying $(p-p_c)W^{1/\nu}=0.064$], which are collapsed to the lower curve, showing scaling to high precision.

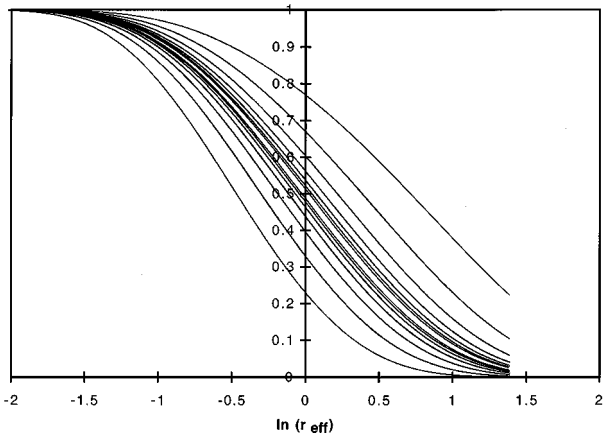

FIG. 8. Plot as in Fig. 7 but for all eight values of p and four values of W, with the 32 different plots falling on 14 distinct curves with (from bottom to top) $(p-p_c)W^{1/\nu}$ = 0.304 437, 0.181 019, 0.107 635, 0.064, 0.038 055, 0.022 627, 0.013 454, and continuing with negative values in reverse order. The ratio of these numbers is $2^{3/4}$.

$$\pi_v(H,W)=\pi_v(r)+\delta\pi_v'(r)+\frac{\delta^2}{2}\pi_v''(r)\cdots$$

$$=\pi_v(r)+\left(\frac{h-rw}{W+w}\right)\pi_v'(r)$$

$$+\frac{1}{2}\left(\frac{h-rw}{W+w}\right)^2\pi_v''(r)\cdots. \qquad (4)$$

Here the derivatives on π_v are taken with respect to r, and we assume $p=p_c$. Clearly, this result is analytic in W for a fixed r, containing terms of order $1/(W+w)$, $1/(W+w)^2\ldots$, or equivalently of orders $1/W$, $1/W^2\ldots$. When $r=1$, (4) gives no correction for bond percolation since $h=w$ implies $\delta=0$, but for other systems (such as site percolation on a square lattice) $\delta\neq 0$ and (4) gives $O(1/W)$ corrections even when $r=1$ as seen in [16]. Note that, at $r=1$, we have $\pi_v'(1)=-\pi_v''(1)=-0.520\,246\ldots$ [15].

B. Scaling behavior for $p\neq p_c$

For p away from p_c, one expects $\pi_v(H,W,p)$ to depend universally upon two ratios of the three length quantities H, W, and $\xi\sim A|p-p_c|^{-\nu}$, were ν is the correlation-length exponent ($=4/3$ in two dimensions) and A is a lattice-dependent constant. (From this point on we will not mention finite-size corrections explicitly, although in the analysis of our results we will generally continue to use use $H+h$ and $W+w$ for H and W, respectively.) One could write this expected behavior as $\pi_v^{(1)}(H/W,(p-p_c)W^{1/\nu})$, or as an equivalent but more symmetric form as $\pi_v^{(2)}(H/W,(p-p_c)(HW)^{1/2\nu})$. For convenience we have incorporated the constant A into these two scaling functions, so they are no longer universal [17]. To investigate this expected behavior, we carried out runs at different values of p, and also measured the derivative of π_v with respect to p evaluated at $p_c=\frac{1}{2}$.

Runs were carried out at $p=0.501$, 0.501 682, 0.502 828, and 0.504 757, and at 0.499, 0.498 318, 0.497 171, and 0.495 243. These values were chosen so that $|p-p_c|W^{1/\nu}$ all have the same value (0.064) for $W=256$, 128, 64, and 32, respectively, for each of these two sets of four cases. (Note here we used W rather than $W+w$ to calculate the values of p; including w changes p only slightly.) Approximately 2 000 000 runs were carried out at each value of p.

In Fig. 7 we show the plot of the eight values of p each with the single corresponding value of W such that $|p-p_c|W^{1/\nu}=0.064$. The four runs for $p>0.5$ all collapse on the upper curve, and the four runs for $p<0.5$ all collapse on the lower curve. Deviations from the expected scaling form are nearly imperceptible, even on a much-expanded plot.

In Fig. 8 we plot the data of all 32 curves for these eight values of p and all four values of W. The 32 curves fall on 14 different scaling curves corresponding to 14 different values of $|p-p_c|W^{1/\nu}$. These curves represent the scaling function $\pi_v^{(1)}$ as a function of its first argument with its second argument fixed to 14 different values. No corrections to scaling, other than the use of $r_{\rm eff}$ for the aspect ratio, were necessary to make a precise collapse.

While the data collapse shown in these two figures is expected according to the simple scaling arguments, this is the first time that such behavior has been shown explicitly as a function of r (except for the case $p=p_c$, which was given in [12,13]). Previous studies of scaling (i.e., [9–11,19]) have generally dealt with a fixed value of r and variable p — that is, the behavior of $\pi_v^{(1)}$ with respect to its second variable. Note that scaling in a different system has been studied by Berche *et al.* [35].

C. Determination of $(\partial\pi_v/\partial p)_{p_c}$

As a second approach to demonstrate scaling, and to test for finite-size corrections, we considered the derivative of π_v with respect to p evaluated at p_c. According to the above scaling, one would expect

$$\left(\frac{\partial\pi_v}{\partial p}\right)_{p_c}=(HW)^{1/2\nu}\left(\frac{\partial\pi_v^{(2)}(H/W,y)}{\partial y}\right)_{y=0}, \qquad (5)$$

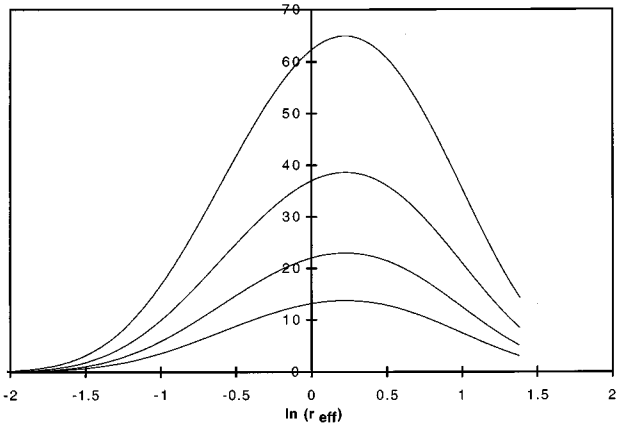

FIG. 9. Plots of $(\partial\pi_v/\partial p)_{p_c}$ determined from simulation data using (7), vs $\ln r_{\rm eff}$, for $W=32$, 64, 128, and 256 (top to bottom).

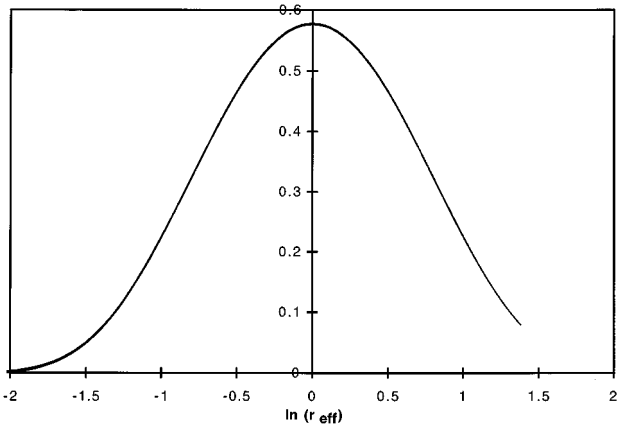

FIG. 10. $(HW)^{-1/2\nu}(\partial\pi_v/\partial p)_{p_c}$ vs $\ln r_{\rm eff}$ for the four values of W, showing collapse of the data in Fig. 9 to a single symmetric scaling curve as predicted by (5).

where $y=(p-p_c)(HW)^{1/2\nu}$, implying that $(HW)^{-1/2\nu}(\partial\pi_v/\partial p)_{p_c}$ should be a function of H/W only.

The quantity $\partial\pi_v/\partial p$ can be found directly in a simulation. Formally, π_v can be written as

$$\pi_v=\sum\ \theta_{\rm top}p^n(1-p)^m, \tag{6}$$

where the sum is over all possible walks, $\theta_{\rm top}$ is unity for those walks that reach the top and zero otherwise, and n and m are the number of occupied and vacant bonds, respectively, in a given hull. Differentiating (6) with respect to p, we find

$$\frac{\partial\pi_v}{\partial p}=\sum\ \left(\frac{n}{p}-\frac{m}{1-p}\right)\theta_{\rm top}p^n(1-p)^m=\left\langle\left(\frac{n}{p}-\frac{m}{1-p}\right)\theta_{\rm top}\right\rangle \tag{7}$$

where the average is weighted by the walk's probability of occurrence, $p^n(1-p)^m$. Now, we approximate the average over all walks by an average over a run of the hull-walk simulation, which generates a sampling of this ensemble. Then $\langle n\,\theta_{\rm top}\rangle$ is simply given by the total number of occupied bonds in walks that hit the top divided by the total number of walks, and $\langle m\,\theta_{\rm top}\rangle$ is given by the total number of vacant bonds for walks that hit the top divided by the total number of walks. This procedure can also be generalized for rectangular systems by keeping track of the quantities n and m for each value of the maximum height, and then accumulating as in π_v, allowing $\partial\pi_v/\partial p$ to be found for all r. Note that the above procedure can in principle be extended for higher derivatives; however, simulations show that it is difficult to get accurate results because of high statistical noise.

In Fig. 9 we show the results for $(\partial\pi_v/\partial p)_{p_c}$ determined from (7) using data from 100 000 000 hulls, plotted as a function of $\ln r_{\rm eff}$ for the four values of W. These curves are of different magnitude, and are not symmetric about $r=1$.

In Fig. 10, we plot these results divided by $(HW)^{1/2\nu}$, and indeed, now find collapse to a single curve as predicted by (5). This curve is symmetric about $\ln r=0$ on this plot which follows from the expected symmetry behavior when $r\leftrightarrow 1/r$. Note that only when the scale factor in the form $(HW)^{1/2\nu}$ is used does a curve with this symmetry follow. In making this plot, we actually used $H+h$ and $W+w$ for H and W, and $r_{\rm eff}$ for r — had we not, the collapse of the curves would not have been so precise. The plot in Fig. 10 is a bell-shaped curve but apparently not quite a Gaussian since a fit gives $(HW)^{-1/2\nu}(\partial\pi_v/\partial p)_{p_c}=0.5763\exp[-0.828(\ln r)^2-0.111(\ln r)^4\ldots]$.

It is interesting to note that $-r(\partial\pi_v/\partial r)_{p_c}$ is also a symmetric bell-shaped but non-Gaussian curve when plotted as a function of $\ln r$, with behavior about $r=1$ given by $0.520\ 246\exp[-0.649\ 106\,(\ln r)^2-0.161\ 994\,(\ln r)^4+0.031\ 382\,(\ln r)^6\ldots]$. (This follows analytically from Cardy's formula using Eq. (11) of [15].) These two functions are evidently different. Note that the area under the curve of $-r(\partial\pi_v/\partial r)_{p_c}$ vs $\ln r$ is exactly unity, which follows by simple integration. It is not clear whether this should also be the case for the function plotted in Fig. 10, although numerically the integral is close to one (1.033 using the above fit).

There is yet a third situation for the crossing problem where non-Gaussian behavior occurs: the quantity $(\partial\pi_v/\partial p)_{r=1}$ for a square $L\times L$ system, as a function of the scaling variable $x=L^{1/\nu}(p-p_c)$, is a symmetric bell-shaped curve of normalized area $(L^{-1/\nu})$, but non-Gaussian with kurtosis $\mu_4/\mu_2^2\approx 3.17$ rather than 3, where μ_n are the central moments [18,19,24]. In this case, non-Gaussian behavior has been proven rigorously by Berlyand and Wehr [36], who show that $\pi_v\sim\exp(-L/\xi)=\exp(-{\rm const}\times x^\nu)$ for $x\gg 1$ (see also Appendix B of [19]). Note that here the independent variable is x or p while in the above two cases it is $\ln r$, so these are quite different functions. If, however, an expression for $\pi_v(r,p)$ for all r and p could be found, then these three different bell-shaped curves could presumably be related to each other.

IV. CONCLUSIONS

We have shown the following.

(1) $\pi_v(H,W,p)$ over a range of H and W (at one value of p) can be found efficiently from a single hull-walk simula-

tion — run many times, of course, to obtain the necessary statistics.

(2) The ratio of the simulation results to the predictions of Cardy's formula grows linearly with increasing $r=H/W$ (with slope $\pi w/3W$) for a finite system of any size W. If, however, the effective aspect ratio $r_{\rm eff}=(H+h)/(W+w)$ with $h\approx w\approx 0.36$ is used in Cardy's formula, then the agreement with theory is obtained to high accuracy. These constants say that the percolation field extrapolates to a boundary 0.18 lattice spacings beyond the edges of the system — both for the free boundaries on the left and right sides, and the conducting boundaries on the top and bottom (which are essentially like free boundaries). These values of h and w are specific to this system; that is, bond percolation on a square lattice with a rectangular boundary and open boundary conditions on the sides.

(3) The introduction of $r_{\rm eff}$ for r introduces analytic finite-size corrections to π_v; no correction term of the type $L^{-\vartheta_1}$ proposed by Aharony and Hovi [17] appears to be necessary to fit the simulation results. However, we did not make a systematic investigation into the finite-size corrections to unequivocally rule out such a term.

(4) For $p\neq p_c$, the scaling form $\pi_v(H,W,p)=\pi_v^{(1)}(H/W,(p-p_c)W^{1/\nu})=\pi_v^{(2)}(H/W,(p-p_c)(HW)^{1/2\nu})$ was precisely verified using eight different values of p and four values of W, for H taking on all values $\leqslant 4W$.

(5). The derivative $(\partial\pi_v/\partial p)_{p_c}$ for all r was also found directly from the hull-walk simulation. Its behavior also verifies scaling and leads to a symmetric non-Gaussian bell-shaped curve when divided by $(HW)^{1/2\nu}$ and plotted as a function of $\ln r$.

For different types of percolation systems and different boundary conditions on the sides, one would expect that (2) remains valid, but that the constants h and w will vary. Indeed, for site percolation on a square lattice with rectangular boundaries and free boundaries on the sides, we find that h and w differ from each other, implying by (4) that $\pi_v(L,L,p_c)$ differs from 1/2 by a term proportional to $1/L$, as was found numerically in [16]. For periodic boundary conditions on the left and right sides, one would expect that w should be zero, but that an offset constant h will still be needed in the vertical direction because of the effectively open boundary, so consequently these systems are *not* free of such analytic corrections as suggested by Hovi and Aharony [19]. Preliminary results verify this with $h\approx 0.39$ and $w=0$. A system that may be free of analytic corrections due to lattice offsets is one that is periodic in *both* directions, as recently considered by Hu and co-workers [10,37]. Because there is no boundary to the system anywhere, and evidently no place for an extrapolation length to enter, corrections should be of higher order. Further discussion of these points will be given in future papers.

ACKNOWLEDGMENTS

This material is based upon work supported by the U.S. National Science Foundation under Grant No. DMR-9520700.

APPENDIX: RANDOM NUMBER GENERATOR USED

The random number generator used for this work was the shift-register sequence generator [38] based upon the recursion $x_n=x_{n-471}\oplus x_{n-1586}\oplus x_{x-6988}\oplus x_{n-9689}$, where the $\oplus$ is the exclusive-or operation (addition modulo two) carried out on each bit of the integers x_n independently. This four-tap generator is equivalent to choosing every seventh result (7-decimation) from the two-tap generator $x_n=x_{x-471}\oplus x_{n-9689}$, and is of the same maximum cycle length, $2^{9689}-1$, as the undecimated generator. The numbers generated from this generator have a built-in five-point correlation over a span of 9689 determined directly by the generator's taps, and four- and three-point correlations with significantly greater spreads [39].

At first the simulations were carried out using the more compact generator $x_n=x_{n-11}\oplus x_{n-39}\oplus x_{x-95}\oplus x_{n-218}$ which derives from a 7-decimation of $x_n=x_{x-11}\oplus x_{n-218}$, but we found systematic errors for $H=W$ (where we know that π_v should be exactly 1/2) that appeared to grow linearly with increasing W. For $W=256$ the observed crossing probability was $0.500\,30\pm 0.000\,05$ for $N=100\,000\,000$ runs. A study of different generators showed that this systematic error diminishes rapidly with increasing size (maximum offset) of the generator, and by size 300 for four-tap generators, errors could not be observed in a reasonable amount of computer time.

To be (presumably) completely safe, we used a four-tap generator of the much larger size 9689 in this work. While this generator requires a large array to store previous members (we used a list of size 16 384 to make the coding simpler), it is still fast and simple to program.

Note that, for smaller generators, and especially two-tap ones such as the notorious [39–42] generator $x_n=x_{x-103}\oplus x_{n-250}$ of Kirkpatrick and Stoll [43], the error in π_v was immediately obvious (giving $\pi_v=0.441$ for $H=W=512$). Two-tap generators have inherent asymmetric three-point correlations over the span of the generator size (250 in this case), and evidently these short-ranged correlations are very detrimental for this problem. Indeed, the simulation carried out here appears to be a particularly good test for the shift register sequence random number generator.

[1] J. Bernasconi, Phys. Rev. B **18**, 2185 (1978).

[2] A. P. Young and R. B. Stinchcombe, J. Phys. C **8**, L535 (1975).

[3] S. Kirkpatrick, in *Proceedings of the Les Houches Summer School on Ill-Condensed Matter* (North-Holland, Amsterdam, 1980).

[4] P. J. Reynolds, H. E. Stanley, and W. Klein, Phys. Rev. B **21**, 1223 (1980).

[5] D. Stauffer and A. Aharony, *An Introduction to Percolation Theory*, revised 2nd ed. (Taylor and Francis, London, 1994).
[6] C.-K. Hu, Phys. Rev. B **46**, 6592 (1992).
[7] C.-K. Hu, Phys. Rev. B **51**, 3922 (1995).
[8] C.-K. Hu and J.-A. Chen, J. Phys. A **27**, L813 (1994).
[9] C.-K. Hu and J.-A. Chen, J. Phys. A **28**, L73 (1995).
[10] C.-K. Hu, C.-Y. Lin, and J.-A. Chen, Phys. Rev. Lett. **75**, 193 (1995).
[11] R. Monetti and E. Albano, Zeit. Phys. B **90**, 351 (1993).
[12] R. P. Langlands, C. Pichet, Ph. Pouliot, and Y. Saint-Aubin, J. Stat. Phys. **67**, 553 (1992).
[13] R. Langlands, P. Pouliot, and Y. Saint-Aubin, Bull. Am. Math. Soc. **30**, 1 (1994).
[14] J. L. Cardy, J. Phys. A **25**, L201 (1992).
[15] R. M. Ziff, J. Phys. A **28**, 1249 (1995), **28**, 6479 (1995).
[16] R. M. Ziff, Phys. Rev. Lett. **69**, 2670 (1992).
[17] A. Aharony and J.-P. Hovi, Phys. Rev. Lett. **72**, 1941 (1994).
[18] R. M. Ziff, Phys. Rev. Lett. **72**, 1942 (1994).
[19] J.-P. Hovi and A. Aharony, Phys. Rev. E **53**, 235 (1996).
[20] F. Yonezawa, S. Sakamoto, and M. Hori, Phys. Rev. B **40**, 636 (1989).
[21] M. Sahimi and H. Rassamdana, J. Stat. Phys. **78**, 1157 (1995).
[22] U. Gropengiesser and D. Stauffer, Physica A **210**, 320 (1994).
[23] D. Stauffer, J. Adler, and A. Aharony, J. Phys. A **27**, L475 (1994).
[24] U. Haas, Physica A **215**, 247 (1995).
[25] R. M. Ziff, P. T. Cummings, and G. Stell, J. Phys. A **17**, 3009 (1984).
[26] P. Grassberger, J. Phys. A **19**, 2675 (1986).
[27] J. M. F. Gunn and M. Ortuño, J. Phys. A **18**, L1095 (1985).
[28] T. W. Ruijgrok and E. G. D. Cohen, Phys. Lett. A **133**, 415 (1988).
[29] R. M. Ziff, Physica D **38**, 377 (1989).
[30] P. Grassberger, J. Phys. A **25**, 5475 (1992).
[31] A. Malakis, J. Phys. A **8**, 1885 (1975).
[32] J. W. Lyklema, J. Phys. A **18**, L617 (1985).
[33] An annotated version of the program and output files can be obtained by e-mail from rziff@engin.umich.edu.
[34] R. M. Ziff, J. Stat. Phys. **65**, 1217 (1991).
[35] B. Berche, J.-M. Debierre, and H.-P. Eckle, Phys. Rev. E **50**, 4542 (1994). R. M. Ziff, J. Stat. Phys. **65**, 1217 (1991).
[36] L. Berlyand and J. Wehr, J. Phys. A **28**, 7127 (1995).
[37] C.-K. Hu, Phys. Rev. Lett. **76**, 3875 (1996).
[38] S. Golomb, *Shift Register Sequences* (Aegean Park Press, Laguna Hills, CA, 1982).
[39] R. M. Ziff (unpublished).
[40] A. M. Ferrenberg, D. P. Landau, and Y. J. Wong, Phys. Rev. Lett. **69**, 3382 (1992).
[41] P. Grassberger, Phys. Lett. A **181**, 43 (1993).
[42] I. Vattulainen, T. Ala-Nissila, and K. Kankaala, Phys. Rev. Lett. **73**, 2513 (1994).
[43] S. Kirkpatrick and E. P. Stoll, J. Comput. Phys. **40**, 517 (1981).